Fracture of Laminated Bamboo and the Influence of Preservative Treatments

Fracture of Laminated Bamboo and the Influence of Preservative Treatments

Thomas P S Reynolds[a,*], Bhavna Sharma[b], Erik Serrano[c], Per-Johan Gustafsson[c], Michael H Ramage[d],

[a]*Institute for Infrastructure and Environment, School of Engineering, University of Edinburgh*
[b]*Department of Architecture and Civil Engineering, University of Bath*
[c]*Department of Construction Sciences, Lund University*
[d]*Department of Architecture, University of Cambridge*

Abstract

Treated bamboo can be made into large, durable structural elements which have the potential to become a transformative large-scale building material, but the fracture behaviour which determines their ultimate strength in various loading scenarios has not been studied. Laminated bamboo is a promising structural engineered bamboo material, and is generally made from bamboo treated to improve its durability. Studies into the structural behaviour of laminated bamboo indicate that different preservative treatments affect the structural properties of the composite differently, with conflicting evidence from tests in different load orientations. This study uses fracture mechanical testing and microscopy to develop an understanding of the fracture mechanics of engineered bamboo, and explains why the properties of the composite under tension, compression and bending may be affected differently by the treatment processes. Two types of treated Moso bamboo are studied alongside the same material with minimal processing. The treated material had gone through one of two commercial processes: bathing in a hydrogen peroxide bleach solution, or treatment by pressurised steam (described as caramelised). The results show that the critical strain energy release rate in the caramelised material is much lower than that in the bleached, and the fracture behaviour of the bleached material is closer to that of the raw bamboo. Fracture experiments included Mode I and Mode II fracture with cracks progressing parallel to the grain, and Mode I fracture with a crack progressing perpendicular to the grain. The results shed new light on the strength of structural-size elements.

Keywords: Laminated bamboo, nonlinear fracture mechanics, bleached, caramelised and carbonised bamboo

1. Background

Woody bamboo species such as Moso (*Phyllostachys pubescens*) produce material with promising structural behaviour [1], and they grow extremely fast: after 40 days, it has reached its full height of around 10m, put on up to 17kg of biomass and stored up to 8kg of carbon [2]. Moso represents 70% of the bamboo cover in Asia [3].

Bamboo is an anisotropic material, with higher stiffness and strength in the grain direction, along the axis of the stem, than in the orthogonal directions. Like some other plant materials, it displays a yield point, beyond which irreversible deformation occurs at a lower stiffness than before yield [4]. In plants, this behaviour is thought to derive from the mobile bonds between hemicelluloses and cellulose fibrils [5, 6]. When loaded in tension, bending or shear, bamboo ultimately

*Corresponding author

fails by brittle fracture, with cracks progressing readily in the grain direction as cells are prised apart from one another [7], or less easily across the grain, which requires cracking of the long, thin fibre cells [8]. The fracture properties thus vary strongly with the orientation of the crack. The crack orientations are defined in this paper as shown in Figure 1Notation for crack orientation in the bamboo culmfigure.1.

None of the previous studies of fracture mechanics of bamboo [7, 8, 9, 10, 11] have yet addressed laminated bamboo. Laminated bamboo is a material formed by gluing strips cut from the culm wall, which can form structural elements such as beams or columns with large cross-section. Fracture in laminated bamboo has some key differences to fracture in raw full-culm bamboo. First, because large cross-sections may be formed by gluing strips taken from the culm, crack orientations, and modes of fracture, may occur which would not readily form in the culm wall. In laminated bamboo, for example, a Mode I radial-longitudinal (RL) crack may form and progress (see Figure 1Notation for crack orientation in the bamboo culmfigure.1). Second, commercially-produced laminated bamboo is made using material which has been through a preservative process to remove or denature the sugars which promote insect and microbial decay. Here, we study material which has been treated by either caramelisation (thermal treatment with steam) or bleaching.

In bamboo, as in other plant stems, most notably wood, fracture behaviour is highly anisotropic, and depends on the cellular microstructure of the material. The extensive literature on fracture of wood holds lessons for the study of fracture in bamboo, and so is reported here alongside the more limited literature on the fracture of bamboo.

The nature of fracture surfaces in bamboo can be studied through Scanning Electron Micrograph (SEM) images [7]. As a Mode I crack progresses across the grain under tensile loading parallel to grain, in the LR or LT orientation, fibre cracking occurs [8], but there is also substantial progression of the fracture surface in the parallel-to-grain RL or TL directions as the crack moves between preferential locations for fibre cracking. This arrest and reinitiation of the crack, along with the high strength of the fibres, leads to a high fracture toughness in this mode.

In wood, Schniewind and Pozniak [12] argue that it is not possible to measure a true fracture toughness in the RL or TL orientation, since a crack cannot be caused to progress perpendicular to the grain without substantial deviation. The tensile failure of a woody material does, however, require crack growth in this direction, however tortuous the path of the crack must be, and so some measure of the resistance to that crack growth is useful. It may not be considered a pure Mode I fracture, and perhaps includes fracture surfaces in other modes.

Ashby et al. [13] measure fracture in wood for cracks running both parallel and perpendicular to the grain, and find a factor of ten difference in the apparent fracture toughness. Amada and Untao [8] measure the Mode I critical stress intensity factor for crack growth in this orientation in Moso bamboo, and compare this toughness with values for wood presented by Ashby et al. [13]. Even at the weaker nodal zones, the toughness of the bamboo is more than double that of Douglas fir, which had the highest perpendicular-to-grain fracture toughness of the woods documented by Ashby et al. [13].

Ashby et al. [13] and Amada and Untao [8] use the critical stress intensity factor as the measure of fracture toughness. Stanzl-Tschegg and Navi [14] prefer fracture energy on the basis that it can express effects such as crack bridging, which consume energy in addition to that used in forming the new fracture surface. The complete force-displacement response for loading and unloading can be used to compute a fracture energy which includes that consumed by crack tip plasticity. This measurement can be adjusted to allow for fibre bridging effects [15].

Shao et al. [16] observe that Mode I crack growth parallel to the grain can be simpler than growth perpendicular to grain, as the crack proceeds along a plane at the interface between cells, with little bridging behind the crack front. This may make this mode more amenable to the tech-

niques of linear elastic fracture mechanics. In contrast, in Mode II fracture of wood, it is seen that fibres bridge the crack, leading to an increased fracture toughness for elongation of a mode II crack than for its initiation [17].

Thermal modification of wood has a large effect on fracture toughness. Reiterer and Sinn [18] treated spruce in an autoclave for 24 hours at temperatures between 160 and 172 °C and pressures between 3.6 and 5.7 bar, leading to a reduction in fracture toughness of 50-80%. In beech, Stanzl-Tschegg and Navi [14] report experiments by Beikircher showing a substantial reduction as a result of treatment for four hours at 180°C. Majano-Majano et al. [19] show that the stress intensity factor and fracture toughness reduce in thermally-modified beech and ash treated at 180°C, 200°C or 230°C. They also measured and controlled moisture content, since the equilibrium moisture content at given atmospheric conditions varies with the heat treatment. They found that although the measured fracture properties varied with moisture content, there was a larger variation due to heat treatment. Thermal modification has been seen to have different effects in the different perpendicular-to-grain orientations [20]. Yin et al. [21] used FTIR spectroscopy to show that the thermal modification of wood had degraded the main hemicellulose, glucomannan. The temperature used for caramelisation of bamboo is lower than in Yin et al.'s [21] study, but given the similar cell-wall molecular architecture in wood and bamboo, there is potential to see a similar reduction in bamboo. Indeed, [23] measure an 18% drop between raw Moso bamboo and the caramelised material used in the present study.

We are not aware of any study into the effect of bleaching on the mechanical properties of wood. Sharma et al. [22] tested bleached Moso bamboo under a variety of mechanical loading conditions. They did not test untreated bamboo, but rather compared the bleached and caramelised materials. The bleaching process has the potential to degrade the lignin in the bamboo, but may not do so substantially in the timescale used in this process.

In this study, we measure fracture toughness in each of the three modes of fracture observed in the failure of beams and connections in laminated bamboo: crack growth parallel to grain in Mode I, perpendicular to grain in Mode I and parallel to grain in Mode II. This work builds on the understanding of the chemical composition [23] and interface properties [24] of the same commercially-produced preservative-treated material.

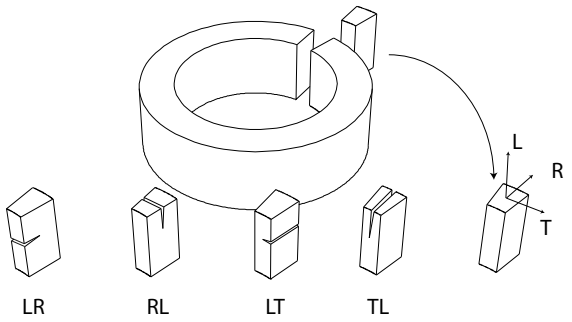

Figure 1: Notation for crack orientation in the bamboo culm

2. Materials and Methods

Figure 1Notation for crack orientation in the bamboo culmfigure.1 shows the notation for defining the crack orientations in an annular segment taken from the bamboo culm. This study focused on fracture which was either normal to, or proceeded in, the longitudinal direction, which is the primary load-carrying direction of the material in structural use.

The fracture tests used commercially-produced laminated bamboo sheets, branded as Plyboo, and untreated Moso bamboo (*Phyllostachys pubescens*) strips glued to form similar sheets using polyurethane adhesive. The material for the sheets was also Moso bamboo, and it had been treated for preservation through one of two commercial processes: by bleaching or caramelisation. In general for bleaching, strips of bamboo are soaked in a bath of hydrogen peroxide solution at approximately 70-80°C. In caramelisation, the strips are treated with steam at approximately 120-130°C. The moisture contents of the specimens were measured after testing by the oven dry method [25]. A detailed study of the chemical composition of these materials after treatment is presented by Sharma

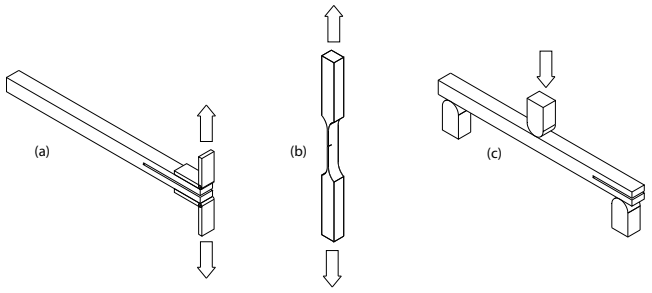

Figure 2: Geometry of test specimens for (a) the double cantilever beam test, (b) the dogbone tensile test and (c) the end-notched flexure test

et al. [23]. The 19mm-thick sheets were cut to form specimens for measurement of the fracture properties of the material.

Raw bamboo specimens were manufactured by taking strips from the culm wall of an untreated Moso bamboo culm. The specimens were taken from near the base of the culm, but excluded the very closely spaced nodes and curvature at the very base, by cutting at the first node with a spacing of more than 150mm. The culm wall thickness allowed prismatic strips between 5mm and 7mm thick and 20mm wide to be produced by cutting and planing to remove the curved surface. These were then glued using a one-component polyurethane adhesive (Purbond HB S309). Approximately 180g/m^2 was applied, although this was difficult to precisely control with these small specimens, and specimens were hand clamped to give a tight fit, and left clamped for at least 12 hours. The specimens were then planed to form 19mm by 19mm square sections.

The tests carried out were:

- tensile loading of dogbone specimens, causing Mode I fracture in the LR orientation;
- a double-cantilever beam test giving Mode I fracture in the RL and TL orientations; and
- end-notched flexure of beams, causing Mode II fracture in the RL and TL orientations.

The crack in the dogbone specimen was therefore loaded in Mode I, with the direction of growth perpendicular to the grain. In the end-notched flexure specimen, the load was Mode II with crack growth parallel to the grain. In the perpendicular-to-grain splitting specimen, the loading was Mode I, with the direction of crack growth parallel to the grain.

Table 1: Number of specimens for each test method

	Raw	Bleached	Caramelised
Mode I LR	-	5	4
Mode I RL	3	3	3
Mode I TL	3	3	3
Mode II RL	3	8	8
Mode II TL	3	6	7

The number of specimens tested is described in full in Table 1Number of specimens for each test methodtable.1. It should be noted that for the Mode I RL and Mode I TL specimens, multiple measurements of fracture toughness were possible as the crack grew and arrested. For each type of specimen, a crack was inserted using a razor blade. In the dogbone specimens, this crack was made at the centre of the 2mm-thick region, and in the other specimens, it was made at the root of a 1.5mm cut.

The Mode I LR specimens were formed by cutting 19mm by 15mm sections, 200mm long, and using a router and template to cut them into a dogbone shape as shown in Figure 2Geometry of test specimens for (a) the double cantilever beam test, (b) the dogbone tensile test and (c) the end-notched flexure testfigure.2, with a minimum dimension of 2mm by 19mm.

The specimens for end-notch flexure were 19mm by 19mm by 300mm, with a 1.5mm wide cut in one end. A 1.5mm thick PTFE sheet was placed in the cut to mitigate closure and frictional effects over the support. The method for end-notch flexure was based on ASTM D7905 [26]. A span of 210mm was used, with the position on the supports chosen to give an initial crack length of 60mm.

For parallel-to-grain splitting, Mode I fracture with RL and TL cracks, 19mm by 19mm by 300mm specimens were tested using the test setup in ASTM D5528 [27]. Steel hinges were screwed and glued to the specimen, and a tensile load applied through

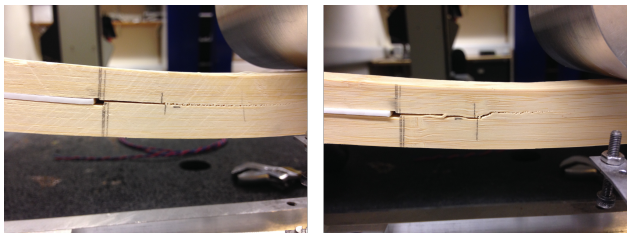

Figure 3: Crack bridging in Mode II fracture of bleached bamboo - the right hand image also illustrates deviation of the crack at a node

them, to allow the ends of the specimen to rotate freely whilst they were pulled apart. A 1.5mm wide cut was made in one end. In each case, the crack grew and arrested so that the fracture toughness could be assessed for at least two crack lengths for each specimen, and as many as eight times in some specimens. The initial crack inserted with a razor blade had its tip approximately 50mm to 80mm from the hinge line. The results therefore correspond to a range of crack lengths between 50mm and 150mm.

The location of the crack tip after propagation was marked and measured under an LED light on the surface on either side of the specimen, and all calculations use the mean of the crack length measured on each side. All displacements were measured along the loading line.

2.1. Linear and non-linear fracture mechanics

Previous fracture mechanical studies of raw bamboo use linear elastic fracture mechanics [8, 9, 10, 7].

Using linear elastic fracture mechanics, the Mode I splitting test may be analysed by the classical Irwin-Kies formula, Equation 1Linear and non-linear fracture mechanicsequation.2.1, which calculates the critical strain energy release rate G_c.

$$G_{I,c} = \frac{P^2}{2b}\frac{dC}{da} \tag{1}$$

P is the applied force, b is the width of the crack, C is the loading head compliance and a is the crack length. The compliance may be measured for each crack length and used to estimate dC/da. The loading rate was initially 2mm/min, and was increased as the crack length increased so that crack growth occurred after approximately 60s.

In Mode II, linear elastic fracture mechanics methods are based on measuring the variation of loading-line compliance as the crack length changes. Davidson and Teller [28], in tests on polymeric matrix composites, determine the variation of compliance with crack length by a pair of tests with different crack length. This variation is assumed to follow the cubic relationship in Equation (2Linear and non-linear fracture mechanicsequation.2.2), where C_0 and m are constants, and m is therefore $dC/d(a^3)$. Substituting this into Equation (1Linear and non-linear fracture mechanicsequation.2.1) gives Equation (3Linear and non-linear fracture mechanicsequa

$$C = C_0 + ma^3 \tag{2}$$

$$G_{II,c} = 1.5m\frac{F_{cr}^2 a^2}{b} \tag{3}$$

The crack lengths in the calibration tests by Davidson and Teller [28] are chosen to be either side of the crack length to be used in fracture tests. In these tests on bamboo, each fracture test included measurement of the compliance at two crack lengths, to provide a measure of the coefficient m from Equations 2Linear and non-linear fracture mechanicsequation.2.2 and 3Linear and non-linear fracture mechanicsequation.2.3, specific to that specimen. A loading head displacement rate of 1mm/min was used, with crack growth beginning after approximately 300s.

Inspection of the force-displacement curve for the fracture tests and of the crack itself give an indication of whether the processes involved in the fracture are predominantly elastic-brittle, or whether dissipative processes or crack bridging occur, either of which may lead to non-linear fracture behaviour. In Mode II, the tests presented here show discontinuous cracks at the surface of the specimen, and crack bridging by large groups of fibres as shown in Figure 3Crack bridging in Mode II fracture of bleached bamboo - the right hand image also illustrates deviation of the crack at a nodefigure.3. There was also evidence of ductile behaviour in the force-displacement diagrams

for some specimens, as shown in Figure 4Force-displacement diagrams for loading and unloading of caramelised material giving Mode I crack growth parallel to grain (left hand axes) and for bleached material in Mode II (right hand axes) with crack growth parallel to grainfigure.4. Methods are therefore required which capture these nonlinear processes.

The total energy dissipated may be estimated by integrating force with respect to displacement around the loading-unloading curve. This integration includes energy dissipation by plasticity, as well as any energy stored in restrained strain due to lack of fit of the fracture surfaces on unloading [15]. Disturbed fracture surfaces and crack bridging are often observed in Mode II, preventing the crack from closing back to its original form. This results in restrained strains in the material, and therefore additional stored energy in the specimen [15]. Because of this, the total work done by the loading head includes this strain energy, and may lead to a substantial overestimate of the critical strain energy release rate. This paper therefore presents the critical strain energy release rate calculated both by linear elastic fracture mechanics, and by integrating the total work done by the loading head.

If the crack propagates in a brittle manner, with insignificant energy dissipation by plasticity, then $G_{I,c}$ or $G_{II,c}$ is equal to the total energy dissipated measured as the integral of force with respect to displacement around the loading-unloading loop, divided by the area of fracture surface created. If other processes lead to nonlinear behaviour, then the two calculations will differ.

Two values of critical strain energy release rate are therefore compared: one calculated as the total work done through integration of the loading-unloading loop (labelled Nn), and one using linear elastic fracture mechanics based on Equations 1Linear and non-linear fracture mechanicsequation.2.1 and 3Linear and non-linear fracture mechanicsequation.2.3 (Labelled Ln).

3. Results and Discussion

The moisture content at the time of testing was different in each type of material, as can be seen in Table 2Moisture contents of specimens measured by the oven dry method (Coefficient of variation in brackets)table.2. Full adsorption and desorption isotherms for the same plyboo material were measured by Sharma et al. [23]. Those results suggest that, for material exposed to the same moisture history, the highest equilibrium moisture content for a given set of conditions should be for the raw bamboo, followed by bleached and then caramelised with the lowest equilibrium moisture content. The results in Table 2Moisture contents of specimens measured by the oven dry method (Coefficient of variation in brackets)table.2 do not follow this pattern. This may be due to differences in atmospheric conditions on the days of the tests, since the raw bamboo was tested at a different time to the bleached and caramelised material. The isotherms presented by Sharma et al. [23] show a change in moisture content of 3 or 4% over the 60 to 70% range of RH to which the specimens may have been exposed in conditioning.

Figure 4Force-displacement diagrams for loading and unloading of caramelised material giving Mode I crack growth parallel to grain (left hand axes) and for bleached material in Mode II (right hand axes) with crack growth parallel to grainfigure.4 shows that for Mode I fracture with an RL crack (splitting along the grain), very little residual displacement remained after fracture, suggesting that the plastic zone at the crack tip is small, and the loading and unloading behaviour is close to linear. The fracture behaviour in Mode I was close to linear elastic, particularly in the case of the caramelised material.

At the other extreme, the Mode II fracture of bleached material by the end-notched flexure method, shown in Figure 4Force-displacement diagrams for loading and unloading of caramelised material giving Mode I crack growth parallel to grain (left hand axes) and for bleached material in Mode II (right hand axes) with crack growth parallel to grainfigure.4 shows several nonlinear features: evidence of yielding and nonlinear de-

Table 2: Moisture contents of specimens measured by the oven dry method (Coefficient of variation in brackets)

	Moisture Content	Density (kg/m^3)
Raw	8.45% (0.029) n=6	618 (0.168)
Bleached	9.60% (0.027) n=9	669 (0.044)
Caramelised	7.79% (0.038) n=10	651 (0.038)

formation before crack propagation, residual displacement on unloading, and hysteresis on reloading.

3.1. Mode I LR Crack

As has been observed in previous research [29], bamboo specimens loaded in tension parallel to the grain with LR or LT cracks exhibit substantial crack growth in the longitudinal grain direction. This leads to crack arrest, as the stress concentration at the tip is removed by longitudinal crack growth. An example of this is shown in Figure 5A specimen loaded in tension parallel to the grain, showing the perpendicular-to-grain crack blunted by transverse crack growthfigure.5. Note that the crack does not follow a glue line. After the arrest of the original crack, the remaining intact cross-section of the specimen is loaded as an uncracked cross section in tension. In this sense, the test appears more like a tensile test on a reduced cross section than a fracture test.

The fracture toughness is expressed as the critical strain energy release rate in Figure 6Critical strain energy release rate for an LR crack: geometry and orientation of lamellae shown in inset sketchfigure.6. There is a clear difference between the bamboo treated by the two methods, with the median fracture toughness approximately three times higher in the bleached bamboo than in the caramelised.

The difference in the response of the bleached and caramelised materials may be partly related to their different moisture contents: Chen et al. [30] note the change in fracture surfaces of raw bamboo with moisture content, although Majano-Majano et al. [19] demonstrate that the change in equilibrium moisture content in treated timber only explains some of the change in fracture toughness. The moisture contents shown in Table 2Moisture contents of specimens measured by the oven dry method (Coefficient of variation in brackets)table.2 are in turn caused by the treatment the specimens have undergone, and the higher fracture toughness in the bleached specimens may point to a plasticising effect from the moisture in the cell walls, which is higher in these specimens.

3.2. Mode I RL and TL Cracks

For crack growth parallel to the grain in Mode I, results were obtained for several crack lengths for each specimen. An example of the full set of results for a single specimen is shown in Figure 7Critical strain energy release rate for Mode I fracture for crack growth parallel to grain: full set of results for a single specimen of caramelised material for a TL crackfigure.7. As was generally the case, this specimen showed no clear evidence of systematic variation of fracture toughness with crack length. For the crack length just greater than 140mm an outlier can be observed. These occurred frequently where the crack progressed through a node in one of the lamellae.

The critical strain energy release rate for all specimens is shown in Figure 8Critical strain energy release rate for Mode I fracture for crack growth parallel to grainfigure.8. In all three materials, the fracture toughness calculated by the two methods is almost equal for this mode of fracture. The linear fracture mechanics and total work calculations give very similar results in these tests, and there was no substantial residual displacement observed.

The results show a higher fracture toughness in the raw and bleached materials than the caramelised, whereas the fracture toughness of the raw and bleached materials was similar overall. A higher fracture toughness was recorded whenever the crack was propagating from a position within a node in one of the laminates, as seen in Figure 7Critical strain energy release rate for Mode I fracture for

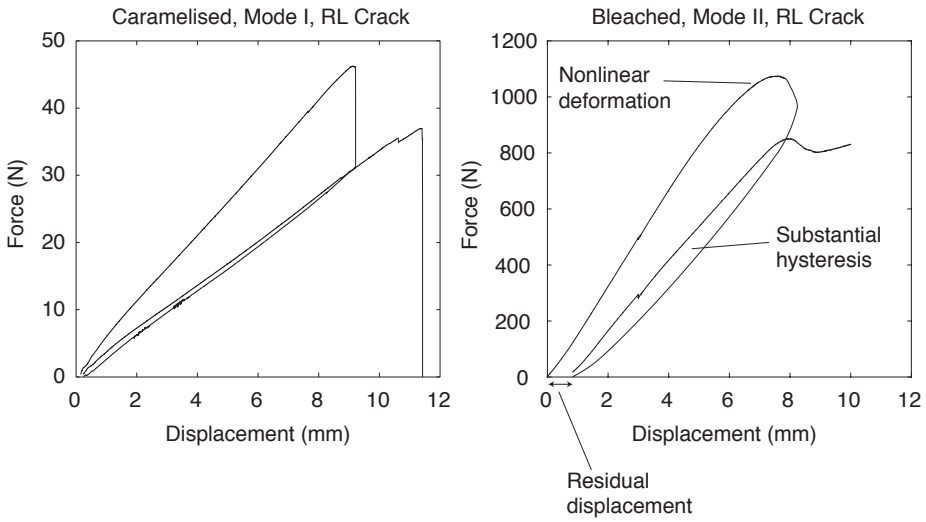

Figure 4: Force-displacement diagrams for loading and unloading of caramelised material giving Mode I crack growth parallel to grain (left hand axes) and for bleached material in Mode II (right hand axes) with crack growth parallel to grain.

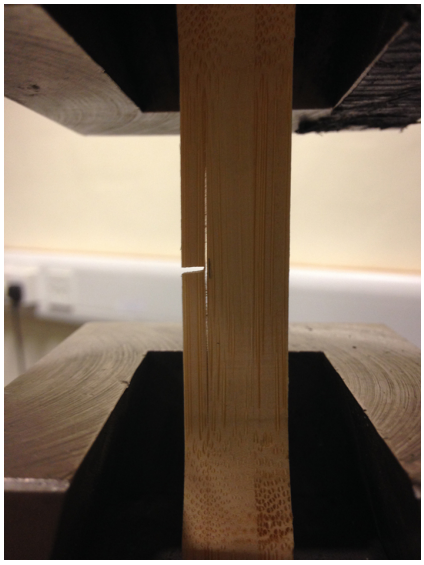

Figure 5: A specimen loaded in tension parallel to the grain, showing the perpendicular-to-grain crack blunted by transverse crack growth

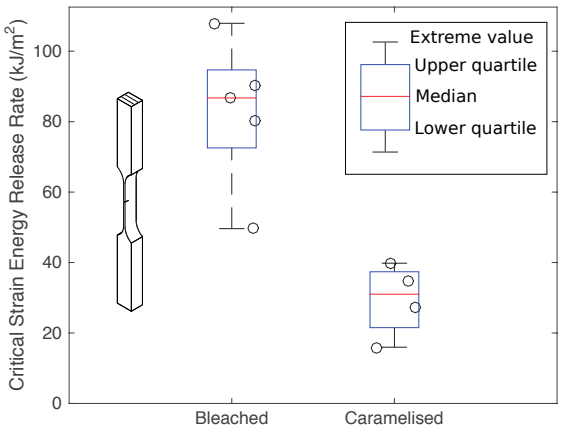

Figure 6: Critical strain energy release rate for an LR crack: geometry and orientation of lamellae shown in inset sketch

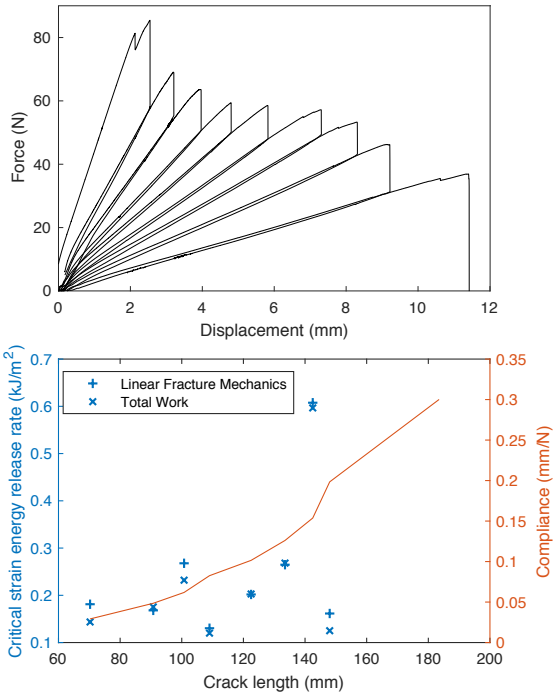

Figure 7: Critical strain energy release rate for Mode I fracture for crack growth parallel to grain: full set of results for a single specimen of caramelised material for a TL crack

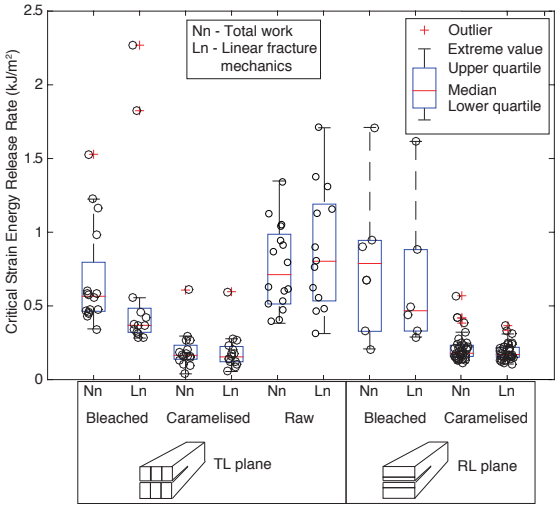

Figure 8: Critical strain energy release rate for Mode I fracture for crack growth parallel to grain

crack growth parallel to grain: full set of results for a single specimen of caramelised material for a TL crackfigure.7. This leads to more scatter in the data than in results in the literature where specimens are taken directly from full-culm bamboo, since they are generally chosen to deliberately include or, more commonly, exclude the nodal region [7, 8, 9, 10, 11].

There is some evidence of a difference in variability between the two orientations, in the bleached material at least - RL has a greater scatter of values than the TL plane. This is due at least in part to the effect of nodes. Fracture toughness was much higher where the crack front was within a node, and because of the orientation of the laminates, it was possible for the RL crack front to be within a node along its entire length. For the TL crack, the effect of the nodes was more distributed since the crack crossed four or five lamellae, and this resulted in lower variability.

3.3. Mode II RL and TL Cracks

Figure 9Critical strain energy release rate for mode II fracture measured by the end notched flexure techniquefigure.9 compares the fracture toughness, expressed as the critical strain energy release rate, for the two parallel to grain crack orientations in Mode II. Again, the toughness measured by the total work done under loading and unloading is compared with that measured by a linear fracture mechanics approach. In this case, Equation 3Linear and non-linear fracture mechanicsequation.2. was used, based on fitting a cubic variation of loading-line stiffness. To a greater extent than the Mode I fracture tests, the two methods give substantially different results for each treatment type. The fracture toughness calculated from the total work done includes the effect of nonlinear deformation at the crack tip, hysteresis and energy stored due to residual displacement.

The fracture toughness was substantially higher in the raw and bleached material than the caramelised material, and again the behaviour of the raw and bleached materials is similar. Correspondingly, the caramelised materials did not show the pronounced non-linear features shown in Figure 4Force-displacement diagrams for loading and unload-

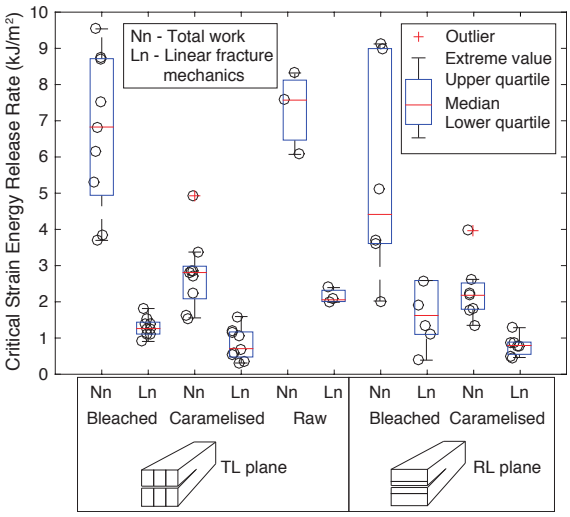

Figure 9: Critical strain energy release rate for mode II fracture measured by the end notched flexure technique

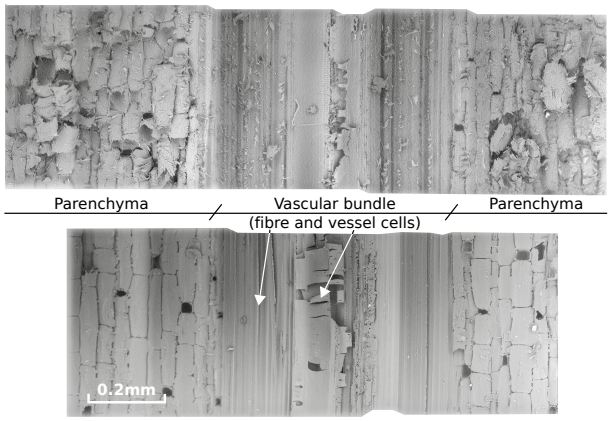

Figure 10: Scanning electron micrograph of Mode I (bottom) and Mode II (top) fracture surface in caramelised bamboo, with the cell types aligned and labelled

ing of caramelised material giving Mode I crack growth parallel to grain (left hand axes) and for bleached material in Mode II (right hand axes) with crack growth parallel to grainfigure.4 for the bleached material.

4. Microscopy

The fracture surfaces were examined through a scanning electron microscope. A substantial difference was observed between those created by Mode I and Mode II fracture. Figure 10Scanning electron micrograph of Mode I (bottom) and Mode II (top) fracture surface in caramelised bamboo, with the cell types aligned and labelledfigure.10 shows both surfaces, including the area where the crack crosses a vascular bundle. In both cases the crack progresses through a vessel, so the images show the fracture surface in the parenchyma, fibre and vessel cells. The surfaces appeared similar for each treatment method.

In Mode I, the parenchyma and fibre cells appear intact and undisturbed, with the fracture surface appearing to have been formed along the middle lamella between the cells. This suggests that little fibre-bridging takes place in this mode, since the fibres immediately adjacent to the fracture surface appear to remain undisturbed. The vessel is split, and the interior of the cell is visible.

In contrast, the Mode II fracture surface shows evidence of tearing of the parenchyma cell walls, and cells are displaced and rotated. In the fibre cells, a difference between the two modes is again visible, with some peeling and roughening of the external surface of the cell wall in Mode II, which is not seen in Mode I. Again the cell wall of the vessel is broken.

A topographic projection in the scanning electron micrograph of the Mode I fracture surface, in Figure 11Scanning elecron micrograph with conventional (left) and topographic projection (right) of Mode I fracture surface in caramelised bamboo, showing the undulating surface of the parenchyma, which interlock with those on the opposite fracture surface, impeding Mode II fracturefigure.11 shows an undulating surface in the parenchyma, showing that the layers of cells interlock in the intact state. While these interlocking cells may be peeled apart by a Mode I crack, leaving the cells in place, this interlock resists the relative sliding of the surfaces in a pure Mode II crack, resulting in displacement and rotation of the parenchyma cells, and tearing of their walls. The fracture energy in Mode II therefore includes both the energy for separation of the parenchyma cells along the middle lamella, and that associated with the other damage to the parenchyma. The damage visible in the micrograph would be expected to constitute part of the nonlinear component of the fracture energy, as it is associated with irreversible

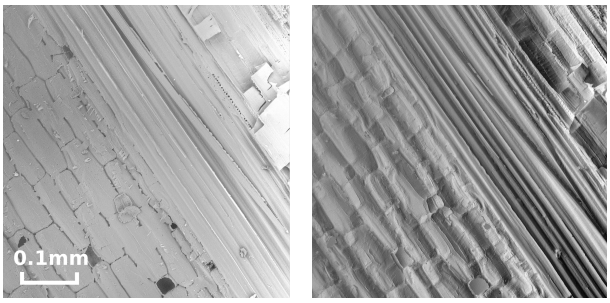

Figure 11: Scanning elecron micrograph with conventional (left) and topographic projection (right) of Mode I fracture surface in caramelised bamboo, showing the undulating surface of the parenchyma, which interlock with those on the opposite fracture surface, impeding Mode II fracture

deformation as well as creation of new surfaces.

The interlocking parenchyma cells may be responsible for the hysteresis and residual displacement in Mode II fracture, as they result in a resistance to the relative movement of the crack faces, which may be considered at a broader scale as a friction force.

5. Relation to strength of structural members

The tests presented in this paper show that there is an order of magnitude difference between the fracture toughness in Mode I for an LR crack, with a median of 85kJ/m^2 based on the total work calculation for the bleached material, and that in Mode II for an RL crack, with a median of 4.5kJ/m^2. The difference is more dramatic using linear elastic fracture mechanics. Another order of magnitude separates the Mode I RL crack, with a median of 0.4kJ/m^2 based on the total work calculation. Despite this dramatic difference in fracture toughness, each of these modes is relevant in the fracture of structural members in laminated bamboo.

Figure 12Fracture surfaces along the crack path in a beam tested to failure in four-point bending by Sharma et al. [1]figure.12 shows the difference in fracture surface along a 3-metre beam specimen of laminated bamboo loaded to failure in four-point bending [1]. A variety of fracture surfaces can be seen. At point 1, the fracture surface is close to planar over substantial areas, with a layer of parenchyma left relatively undisturbed, as seen in the Mode I fracture specimen in Figure 10Scanning electron micrograph of Mode I (bottom) and Mode II (top) fracture surface in caramelised bamboo, with the cell types aligned and labelledfigure.10. At points 2, 3 and 4, individual parenchyma and bundles of parenchma are disturbed and displaced, as seen in the Mode II fracture specimen in Figure 10Scanning electron micrograph of Mode I (bottom) and Mode II (top) fracture surface in caramelised bamboo, with the cell types aligned and labelledfigure.10. Although the crack grows primarily in the grain direction (TL in this beam), its growth from the lower, tension surface at near the loading point, to the middle plane near the supports requires some LT crack growth, as it moves from the presumed point of initiation at the soffit of the beam, towards the neutral axis. This was observed to occur either at joints between the lamellae which make up the beam, or at nodal regions in the bamboo. The image at point 5 looks in the longitudinal direction, and shows bundles of cracked fibres. Also visible are cells running in the plane of the image, which are present at this nodal region, but would not be in the internodal regions.

Sharma et al. [22] show the effect of preservative treatments to glued laminated bamboo on the mechanical properties of structural scale members, and their results are reproduced in Figure 13Strength of structural-scale members tested according to BS EN 408 [31], adapted from [22]figure.13. In tensile loading configurations, which promote the formation and propagation of cracks, the higher fracture toughness of the bleached material results in a higher strength, whereas in compression loading, the higher strength of the specimens of caramelised material points to a higher yield strength, since fracture will not readily occur in these specimens. Similar trends in tension and compression are seen perpendicular to grain.

In flexure, both tension and compression occur in the beam. While the ultimate failure is always by fracture, the interaction between yield in compression and fracture in tension determines the strength of the beam. In the caramelised material, where the tensile and compressive strengths

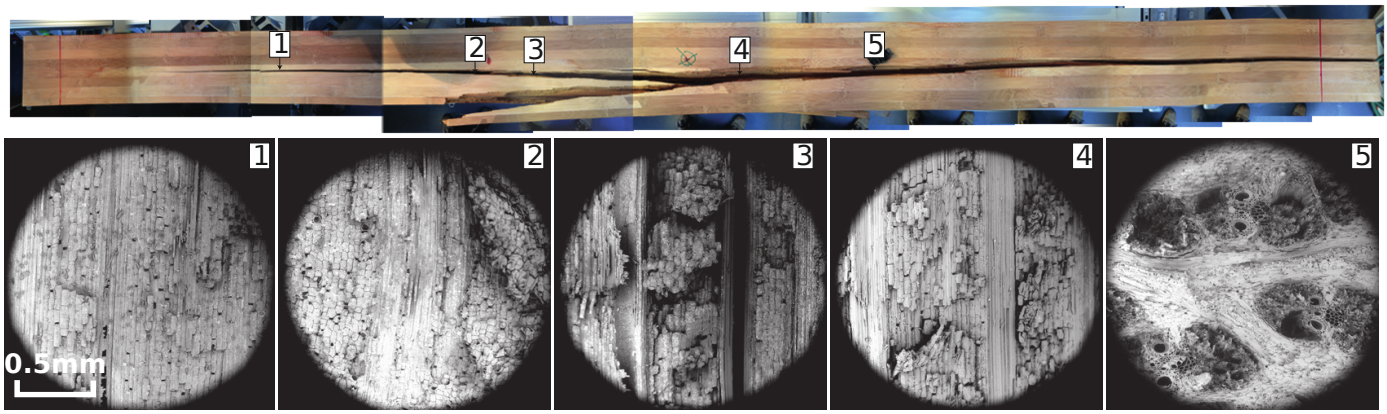

Figure 12: Fracture surfaces along the crack path in a beam tested to failure in four-point bending by Sharma et al. [1]

are approximately equal, the beam might be expected to fail with a near-linear distribution of stress, with fracture occuring at the tension face at around the point that the yield strength is reached at the compression face, and the flexural strength calculated assuming a linear stress distribution falls within the range of the flexural and compressive strengths.

In the bleached material, however, yield would be expected to occur at the compression face at a much lower load than the fracture strength. This does not cause the global failure of the beam, but allows a nonlinear stress distribution to develop, with the neutral axis moving towards the tension face, and increasing the stress at that face until the tensile strength, governed by fracture, is reached. This would explain the fact that the flexural strength based on the assumption of a linear stress distribution is higher than the yield strength in compression, but lower than the pure tensile strength.

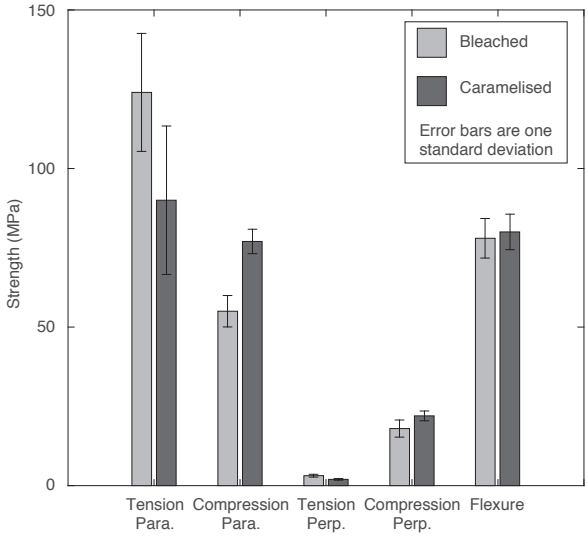

Figure 13: Strength of structural-scale members tested according to BS EN 408 [31], adapted from [22]

6. Conclusion

Fracture in laminated bamboo sections has been investigated, showing the range of crack orientations and modes of fracture which can occur in prismatic sections made up from lamellae cut from the bamboo culm wall. Commercially produced laminated bamboo is treated against decay, and it has been shown that bamboo treated by different methods differs in its fracture properties. Bleached bamboo has higher fracture toughness

than caramelised bamboo in each of the fracture modes tested here, and the difference is greatest for an RL crack. This difference may be at the root of the different strength of specimens made from the two materials, and the fact that bleached bamboo has been observed to be stronger in tension - a load under which fracture governs failure - while caramelised bamboo is stronger in compression - a load under which yield strength governs.

Tests using raw, untreated Moso bamboo laminates showed similar results to the bleached material. This suggests that the bleaching process has little effect on fracture behaviour in these modes, and that the higher temperatures involved in the caramelisation process cause the bamboo to become more brittle. This corresponds to work on the fracture mechanics of wood that has been exposed to high temperatures.

Fracture with LR, RL and TL cracks was investigated, in Modes I and II. Mode I fracture toughness was two orders of magnitude higher for an LR crack than for RL and TL. For RL and TL cracks Mode II fracture toughness was an order of magnitude higher than Mode I. Microscopy shows the physical processes responsible for the differences in fracture energy, and the damage to cells responsible for nonlinear behaviour could be seen. In the ultimate failure of a structural-sized beam, microscopy shows evidence of each of these modes as the crack progresses through the section.

Acknowledgements

This work was supported by a Leverhulme Trust Programme Grant "Natural Material Innovation", and EPSRC Grant EP/K023403/1.

References

[1] B. Sharma, H. Bauer, G. Schickhofer, M. H. Ramage, Mechanical characterisation of structural laminated bamboo, Proceedings of the Institution of Civil Engineers - Structures and Buildings 170 (2016) 1–15, doi:http://dx.doi.org/10.1680/jstbu.16.00061.

[2] T. M. Yen, Culm height development, biomass accumulation and carbon storage in an initial growth stage for a fast-growing moso bamboo (Phyllostachy pubescens), Botanical Studies 57, doi: 10.1186/s40529-016-0126-x.

[3] Z. Ning, Z. Liu, Y. Guo, T. Huang, K. Liu, X. Huang, X. Cao, G. Liu, C. Zhuang, X. Liu, H. Lu, L. Li, Z. Gao, D. Fan, Q. Feng, T. Wang, Y. Lu, K. Miao, W. Tang, T. Hu, L. Yuan, N. Yao, W. Li, Y. Li, Y. Zhao, Q. Zhao, L. Zhang, X. Yang, Z. Jiang, C. Zhu, Y. Liu, Y. Lu, Q. Weng, Z. Liu, Z. Peng, B. Han, C. Zhou, B. Fei, J. Chen, T. Lu, The draft genome of the fast-growing non-timber forest species moso bamboo (Phyllostachys heterocycla), Nature Genetics 45 (4) (2013) 456–461, doi:10.1038/ng.2569.

[4] J. Keckes, I. Burgert, K. Fruhmann, M. Muller, K. Kolln, M. Hamilton, M. Burghammer, S. V. Roth, S. Stanzl-Tschegg, P. Fratzl, Cell-wall recovery after irreversible deformation of wood, Nature Materials 2 (12) (2003) 810–813.

[5] C. M. Altaner, M. C. Jarvis, Modelling polymer interactions of the 'molecular Velcro' type in wood under mechanical stress, Journal of Theoretical Biology 253 (3) (2008) 434–445, ISSN 00225193, doi: 10.1016/j.jtbi.2008.03.010.

[6] L. Köhler, H.-C. Spatz, Micromechanics of plant tissues beyond the linear-elastic range, Planta 215 (1) (2002) 33–40.

[7] M. K. Habibi, Y. Lu, Crack Propagation in Bamboo's Hierarchical Cellular Structure, Scientific Reports 4.

[8] S. Amada, S. Untao, Fracture properties of bamboo, Composites Part B: Engineering 32 (5) (2001) 451–459.

[9] D. Mitch, K. A. Harries, B. Sharma, Characterization of Splitting Behavior of Bamboo Culms, J. Mater. Civ. Eng. 22 (11) (2010) 1195–1199.

[10] F. Wang, Z. Shao, Y. Wu, Mode II interlaminar fracture properties of Moso bamboo, Composites Part B: Engineering 44 (1) (2013) 242–247, doi: 10.1016/j.compositesb.2012.05.035.

[11] R. Ellison, Mode II Fracture Mechanics of Moso Bamboo for Application in Novel Engineering Materials, Batchelor of science, Massachusetts Institute of Technology, URL `http://hdl.handle.net/1721.1/98653`, 2015.

[12] A. Schniewind, R. Pozniak, On the fracture toughness of Douglas fir wood, Engineering Fracture Mechanics 2 (3) (1971) 223–230, doi:10.1016/0013-7944(71)90026-9.

[13] M. F. Ashby, K. E. Easterling, R. Harrysson, S. K. Maiti, The Fracture and Toughness of Woods, Proceedings of the Royal Society of London. Series A, Mathematical and Physical Sciences 398 (1815) (1985) 261–280.

[14] S. E. Stanzl-Tschegg, P. Navi, Fracture behaviour of wood and its composites. A review COST Action E35 2004-2008: Wood machining micromechanics and fracture, Holzforschung 63 (2) (2009) 139–149.

[15] N. Matsumoto, J. A. Nairn, Fracture Toughness of MDF and other Materials with Fiber Bridging, in: Proceedings of the 22nd Annual Technical Conference

of the American Society of Composites, Seattle, WA, USA, ISBN 9781604239669, 19, 2007.

[16] Z.-P. Shao, C.-H. Fang, G.-L. Tian, Mode I interlaminar fracture property of moso bamboo (Phyllostachys pubescens), Wood Science and Technology 43 (5-6) (2009) 527–536, doi:10.1007/s00226-009-0265-2.

[17] H. Yoshihara, Mode II initiation fracture toughness analysis for wood obtained by 3-ENF test, Composites Science and Technology 65 (14) (2005) 2198–2207, doi:10.1016/j.compscitech.2005.04.019.

[18] A. Reiterer, G. Sinn, Fracture behaviour of modified spruce wood: A study using linear and non linear fracture mechanics, Holzforschung 56 (2) (2002) 191–198.

[19] A. Majano-Majano, M. Hughes, J. L. Fernandez-Cabo, The fracture toughness and properties of thermally modified beech and ash at different moisture contents, Wood Science and Technology 46 (1-3) (2012) 5–21, ISSN 00437719, doi:10.1007/s00226-010-0389-4.

[20] P. Tukiainen, M. Hughes, The effect of elevated temperature and high moisture content on the fracture behaviour of thermally modified spruce, Journal of Materials Science 51 (3) (2016) 1437–1444, ISSN 15734803, doi:10.1007/s10853-015-9463-5.

[21] Y. Yin, L. Berglund, L. Salmén, Effect of Steam Treatment on the Properties of Wood Cell Walls, Biomacromolecules 12 (1) (2011) 194–202, ISSN 1525-7797, doi:10.1021/bm101144m.

[22] B. Sharma, A. Gatoo, M. H. Ramage, Effect of processing methods on the mechanical properties of engineered bamboo, Construction and Building Materials 83 (0) (2015) 95–101.

[23] B. Sharma, D. U. Shah, J. Beaugrand, E. R. Janeček, O. A. Scherman, M. H. Ramage, Chemical composition of processed bamboo for structural applications, Cellulose 25 (6) (2018) 3255–3266, doi:10.1007/s10570-018-1789-0.

[24] D. U. Shah, B. Sharma, M. H. Ramage, Processing bamboo for structural composites: Influence of preservative treatments on surface and interface properties, International Journal of Adhesion and Adhesives 85 (May) (2018) 15–22, doi:10.1016/j.ijadhadh.2018.05.009.

[25] CEN, BS EN 13183-2:2002 Moisture content of a piece of sawn timber - Part 1: Determination by the oven dry method, 2007.

[26] American Society for Testing and Materials (ASTM), D7905/D7905M-14 Standard Test Method for Determination of the Mode II Interlaminar Fracture Toughness of Unidirectional Fiber-Reinforced Polymer Matrix Composites, doi:10.1520/D7905, 2014.

[27] American Society for Testing and Materials (ASTM), D5528-01 2001. Standard Test Method for Mode I Interlaminar Fracture Toughness of Unidirectional Fiber-Reinforced Polymer Matrix Composites, doi:10.1520/D5528-13.2, 2014.

[28] B. D. Davidson, S. S. Teller, Recommendations for an ASTM Standardized Test for Determining GIIc of Unidirectional Laminated Polymeric Matrix Composites, Journal of ASTM International 7 (2) (2010) 1–11, doi:10.1520/JAI102619.

[29] T. Tan, N. Rahbar, S. M. Allameh, S. Kwofie, D. Dissmore, K. Ghavami, W. O. Soboyejo, Mechanical properties of functionally graded hierarchical bamboo structures, Acta biomaterialia 7 (10) (2011) 3796–803, doi:10.1016/j.actbio.2011.06.008.

[30] G. Chen, H. Luo, S. Wu, J. Guan, J. Luo, T. Zhao, Flexural deformation and fracture behaviors of bamboo with gradient hierarchical fibrous structure and water content, Composites Science and Technology 157 (2018) 126–133, ISSN 02663538, doi:10.1016/j.compscitech.2018.01.034.

[31] BSI, BS EN 408:2011 Timber structures. Structural timber and glued laminated timber. Determination of some physical and mechanical properties, 2011.